

Supporting Information

Highly Crystalline Lithium Chloride-Intercalated Graphitic Carbon

Nitride Hollow Nanotubes for Effective Lead Removal

Ying Zhou,^a Changzhong Liao,^{*a, b} Yiang Fan,^a Shengshou Ma,^b Minhua Su,^c

Zhengyuan Zhou,^d Ting-Shan Chan,^e Ying-Rui Lu,^e Kaimin Shih^{*a}

^a Department of Civil Engineering, The University of Hong Kong, Pokfulam Road, Hong Kong, HKSAR, China

^b Guangdong Key Laboratory of Integrated Agro-environmental Pollution Control and Management, Guangdong Institute of Eco-Environmental Science & Technology, Guangzhou, China

^c Guangdong Provincial Key Laboratory of Radionuclides Pollution Control and Resources, School of Environmental Science and Engineering, Guangzhou University, Guangzhou, China

^d School of Materials Science and Technology, Jingdezhen Ceramic Institute, Jingdezhen, China

^e National Synchrotron Radiation Research Center, Hsinchu Science Park, Hsinchu, Taiwan, ROC

*Corresponding author:

Professor Kaimin Shih, E-mail: kshih@hku.hk; Tel: +852 28591973; Fax: +852 25595337.

Dr. Changzhong Liao, E-mail: liaocz29@connect.hku.hk

(15 pages including 2 texts, 6 tables and 10 figures)

List of Supporting Information

- Text S1.** Methods and calculations for batch adsorption tests.
- Text S2.** Definitions and calculations of Langmuir and Freundlich models.
- Table S1.** Physicochemical properties of the synthesized g-C₃N₄ and LiCl-intercalated graphitic carbon nitrides.
- Table S2.** Surface element composition of g-C₃N₄ and LiCl-CN-4h before and after Pb adsorption by XPS.
- Table S3.** Kinetic parameters for Pb(II) adsorption on LiCl-CN samples at 298.15K.
- Table S4.** Langmuir and Freundlich Parameters for Pb(II) Adsorption on LiCl-CN-4h.
- Table S5.** Thermodynamic parameters of Pb(II) adsorption on LiCl-CN-4h at various temperatures (298.15K, 308.15K and 318.15K).
- Table S6.** Chemical compositions obtained by EDX for the LiCl-CN samples
- Figure S1.** Crystallinity of the LiCl-CN samples.
- Figure S2.** SEM (a) and TEM (b) images of bulk g-C₃N₄.
- Figure S3.** SEM images of the LiCl-CN-4h sample surface.
- Figure S4.** Elemental mapping of LiCl-CN-4h (a) and bulk g-C₃N₄ (b).
- Figure S5.** XPS high resolution spectra of Li 1s before and after Pb²⁺ adsorption on LiCl-CN-4h.
- Figure S6.** Zeta-potential of bulk g-C₃N₄ and LiCl-CN-4h as a function of pH values.
- Figure S7.** High resolution spectra of C 1s and N 1s before (a and b) and after (c and d) Pb adsorption on LiCl-CN-4h.
- Figure S8.** Infrared spectra of the as-prepared (a) and Pb²⁺-adsorbed LiCl-CN-4h (b).
- Figure S9.** TEM-EDX line-scan profiles of the elements (a), together with the individual element distribution of C (b), N (c), Cl (d) and Pb (e) across the hollow tube after adsorption.
- Figure S10.** Pb L3-edge XANES spectra for samples after Pb²⁺ treatment.

Text S1. Methods and calculations for batch adsorption tests.

The sorption percentage (%) and the adsorption capacity (q_e) were calculated by the following equations:

$$\text{Adsorption (\%)} = \frac{(C_0 - C_e)}{C_0} \times 100\% \quad (1)$$

$$q_e = \frac{(C_0 - C_e) \times V}{m} \quad (2)$$

where C_0 and C_e (mg/L) are the initial and equilibrium concentrations with adsorbents in solution, q_e (mg/g) is the equilibrium adsorption capacity; V (L) is the Pb(II) solution volume and m (g) is the weight of the adsorbents.

To investigate the effect of cation competitiveness on Pb(II) adsorption, 0.01g LiCl-CN powders were added into 50mL solution containing 50 mg/L Pb(II) ions and the competitive cations (including Ca(II) or Mg(II)) with different concentrations. The competitive cation solutions were prepared by calcium nitrate tetrahydrate (99%, Sigma-Aldrich) and magnesium nitrate hexahydrate (99%, Sigma-Aldrich). The testing tubes were then transferred into an incubator shaker and shaken under 200 rpm for 48h, then the equilibrium Pb (II), the final Ca (II) or Mg (II) concentrations were measured accordingly. All the experiment data were the average of the duplicate determinations and the errors were within 5%.

76 **Text S2.** Definitions and calculations of Langmuir and Freundlich models.

77 The as-obtained adsorption data were then fitted to Langmuir and Freundlich models,

78 and the model equations are given as follows:

79 Langmuir model:

80
$$\frac{C_e}{q_s} = \frac{1}{q_{s,max} \times K_L} + \frac{C_e}{q_{s,max}} \quad (3)$$

81 Freundlich model:

82
$$\log q_s = \log K_F + \frac{1}{n} \times \log C_e \quad (4)$$

83 where C_e is the equilibrium concentration ($\text{mg} \cdot \text{L}^{-1}$), q_s is adsorbed Pb(II) per unit weight

84 of sorbents at equilibrium state ($\text{mg} \cdot \text{g}^{-1}$), K_L ($\text{L} \cdot \text{mg}^{-1}$) and K_F ($\text{mg}^{1-n} \text{L}^n \text{g}^{-1}$) are the

85 Langmuir and Freundlich constant, respectively, n is relevant to the adsorption intensity

86 and $q_{s,max}$ (mg g^{-1}) refers to the maximum adsorption capacity of the material.

87

Table S1. Physicochemical properties of the synthesized g-C₃N₄ and LiCl-intercalated graphitic carbon nitrides.

	BET specific surface	Pore volume	Average pore size
	area (m ² /g)	(cm ³ /g)	(nm)
Bulk g-C ₃ N ₄	5.2516	0.0375	24.2161
LiCl-CN-0.5h	16.4695	0.0766	24.9606
LiCl-CN-1h	16.2284	0.0538	23.4909
LiCl-CN-2h	30.2520	0.0731	10.6883
LiCl-CN-4h	36.5378	0.0914	9.9970

Table S2. Surface element composition of g-C₃N₄ and LiCl-CN-4h before and after

	Pb adsorption by XPS					
	C	N	O	Cl	Li	Pb
	(atom.%)	(atom.%)	(atom.%)	(atom.%)	(atom.%)	(atom.%)
g-C ₃ N ₄ -before	42.50	55.25	2.25	---	---	0
g-C ₃ N ₄ -after	49.64	43.42	6.82	---	---	0.12
LiCl-CN-4h before	44.55	35.19	8.72	2.68	8.86	0
LiCl-CN-4h after	43.67	35.76	9.53	2.32	7.68	1.05

97 **Table S3.** Kinetic parameters for Pb(II) adsorption on LiCl-CN samples at 298.15K.

	Pseudo-First-Order			Pseudo-Second-Order		
	k_1	R^2	$q_{1,cal}$	k_2	R^2	$q_{2,cal}$
	(h ⁻¹)		(mg·g ⁻¹)	(g·mg ⁻¹ ·h ⁻¹)		(mg·g ⁻¹)
LiCl-CN-0.5h	1.7226	0.9307	92.03	0.0278	0.9983	95.79
LiCl-CN-1h	2.2169	0.9428	108.34	0.0081	0.9910	123.92
LiCl-CN-2h	2.5465	0.8621	130.60	0.0070	0.9974	151.52
LiCl-CN-4h	3.8988	0.8629	138.43	0.0078	0.9985	160.77

98

99 **Table S4.** Langmuir and Freundlich parameters for Pb(II) adsorption on

100 LiCl-CN-4h.

	Langmuir			Freundlich		
	K_L	$C_{s,max}$	R^2	K_F	n	R^2
	(L·mg ⁻¹)	(mg·g ⁻¹)		(mg ^(1-1/n) L ^{1/n} g ⁻¹)		
298.15K	0.5524	172.41	0.9941	124.39	13.21	0.8200
308.15K	0.4898	208.33	0.9943	110.61	6.33	0.8470
318.15K	1.5666	212.77	0.9982	175.83	19.38	0.7654

101

102

103

104

105

Table S5. Thermodynamic parameters of Pb(II) adsorption on LiCl-CN-4h at various temperatures (298.15K, 308.15K and 318.15K).

ΔH^0 (kJ·mol ⁻¹)	ΔS^0 (J·mol ⁻¹ K ⁻¹)	ΔG^0 (kJ·mol ⁻¹)		
		298.15K	308.15K	318.15K
37.84	149.01	-6.74	-7.69	-9.74

Table S6. Chemical compositions obtained by EDX for the LiCl-CN samples

	C (atom.%)	N (atom.%)	Cl (atom.%)
LiCl-CN-0.5h	44.23	53.87	1.90
LiCl-CN-1h	41.81	55.95	2.25
LiCl-CN-2h	43.29	54.18	2.53
LiCl-CN-4h	45.25	51.81	2.94

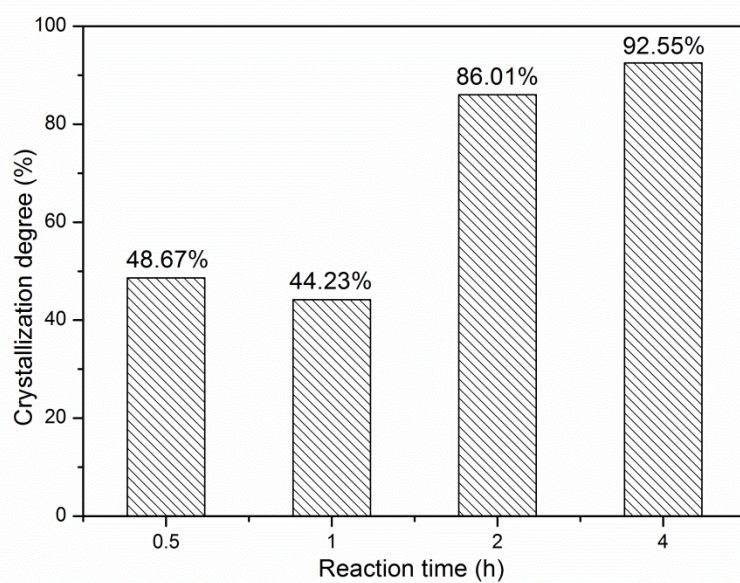


Figure S1. Crystallinity of the LiCl-CN samples.

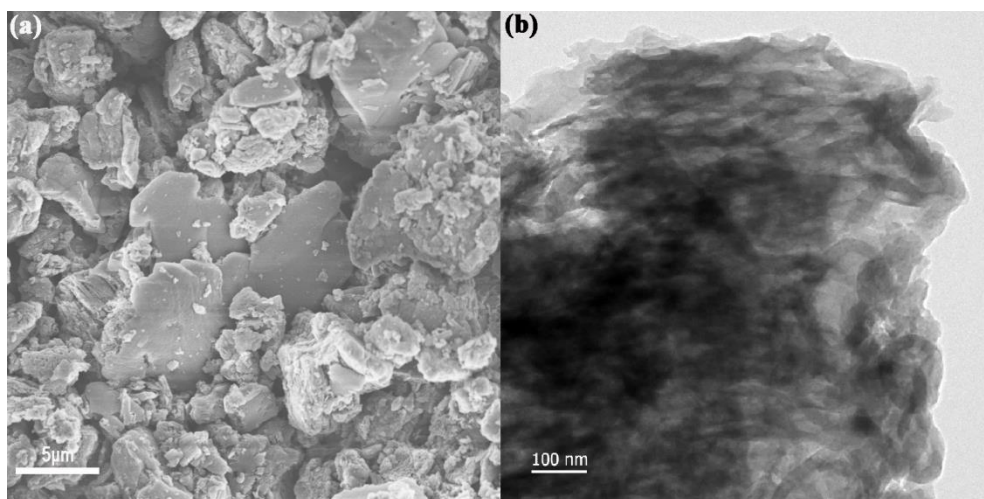


Figure S2. SEM (a) and TEM (b) images of bulk g-C₃N₄.

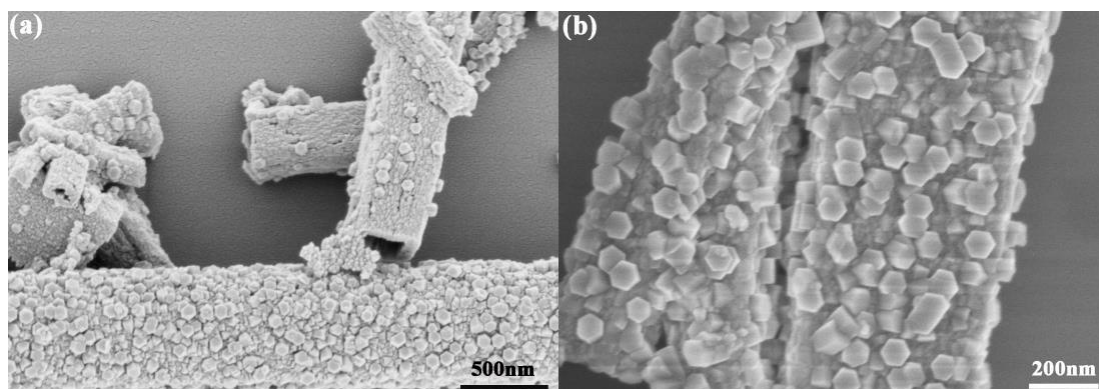


Figure S3. SEM images of the LiCl-CN-4h sample surface.

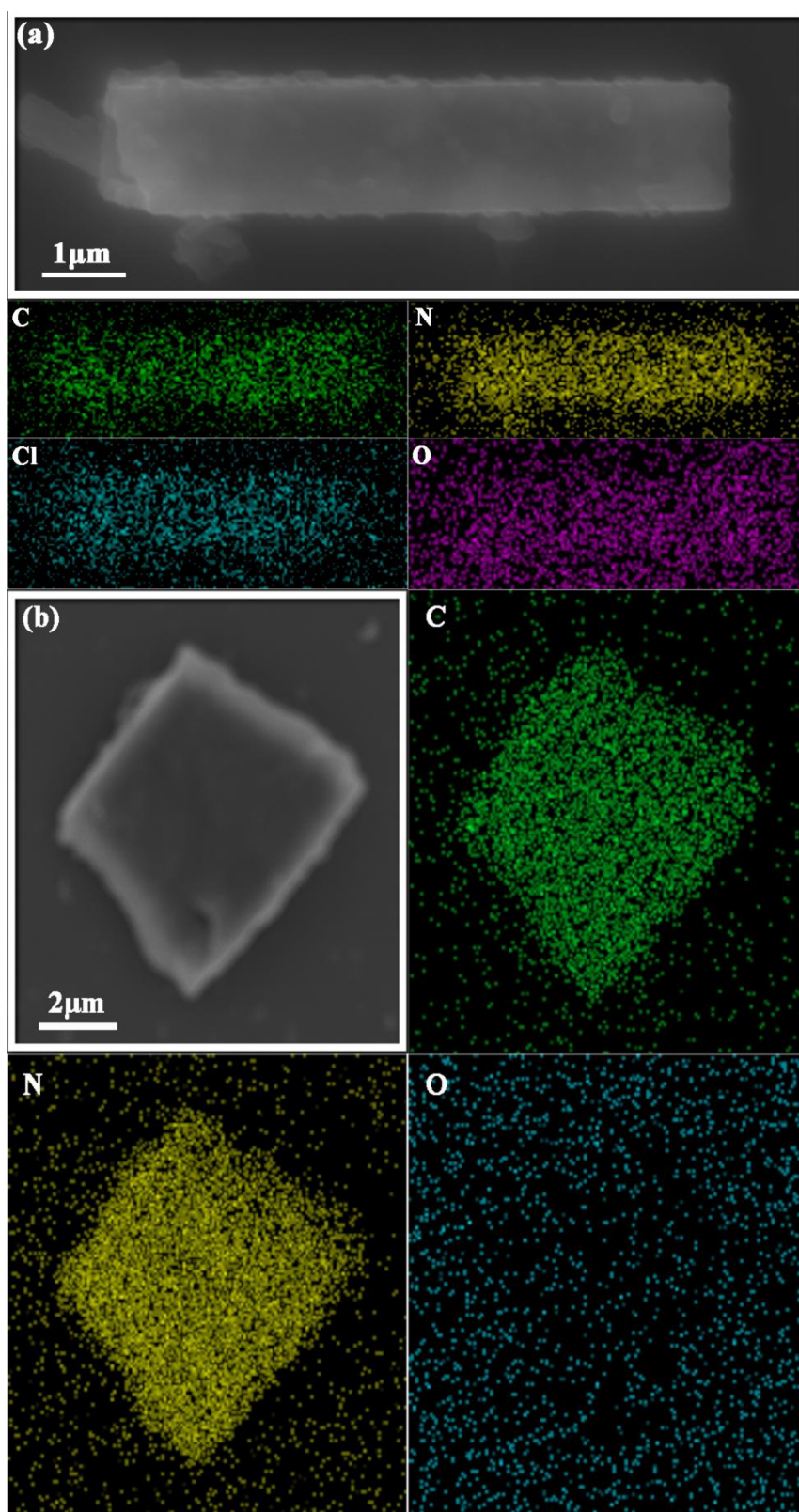


Figure S4. Elemental mapping of LiCl-CN-4h (a) and the bulk g-C₃N₄ (b).

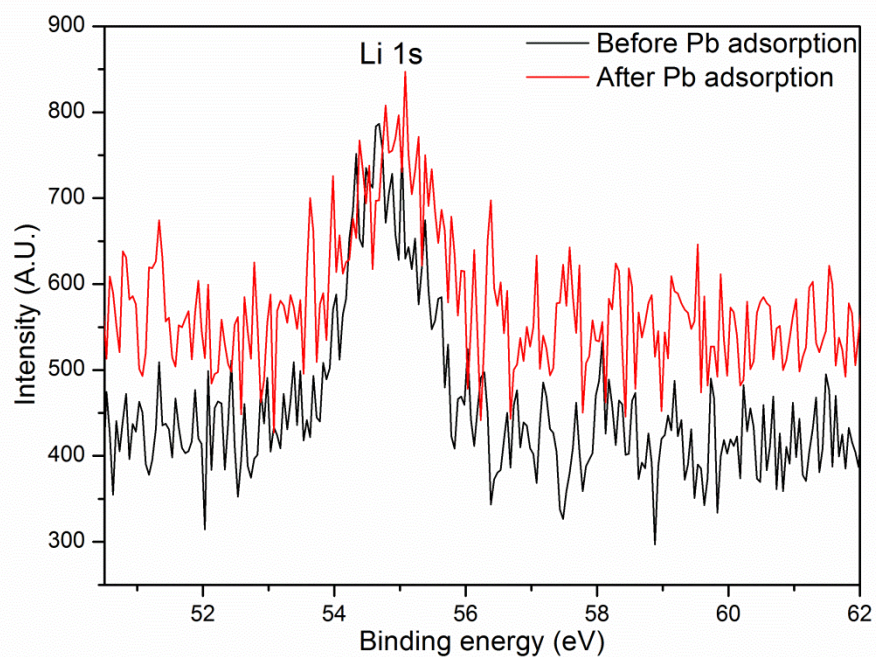


Figure S5. XPS high resolution spectra of Li 1s before and after Pb²⁺ adsorption on LiCl-CN-4h.

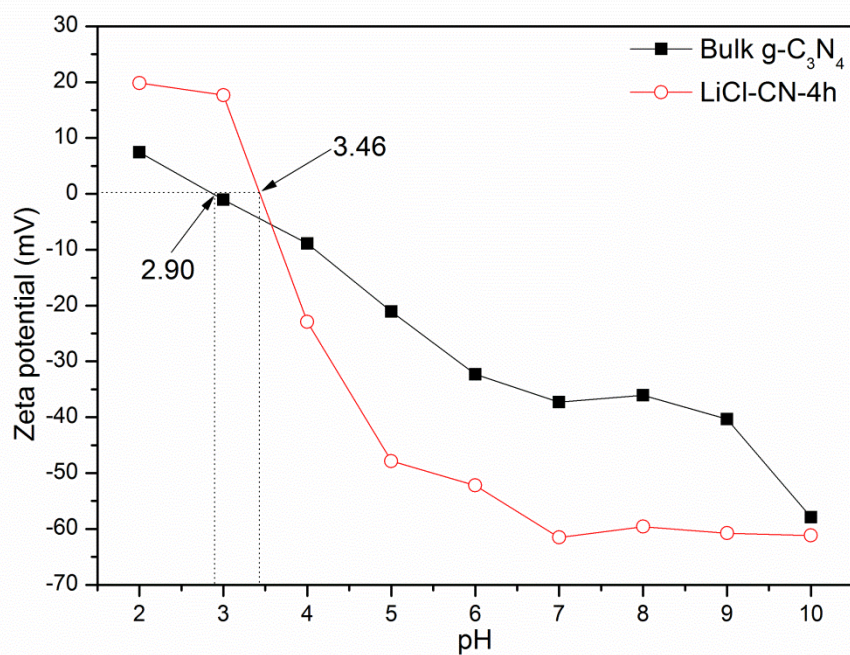


Figure S6. Zeta-potential of bulk g-C₃N₄ and LiCl-CN-4h as a function of pH values.

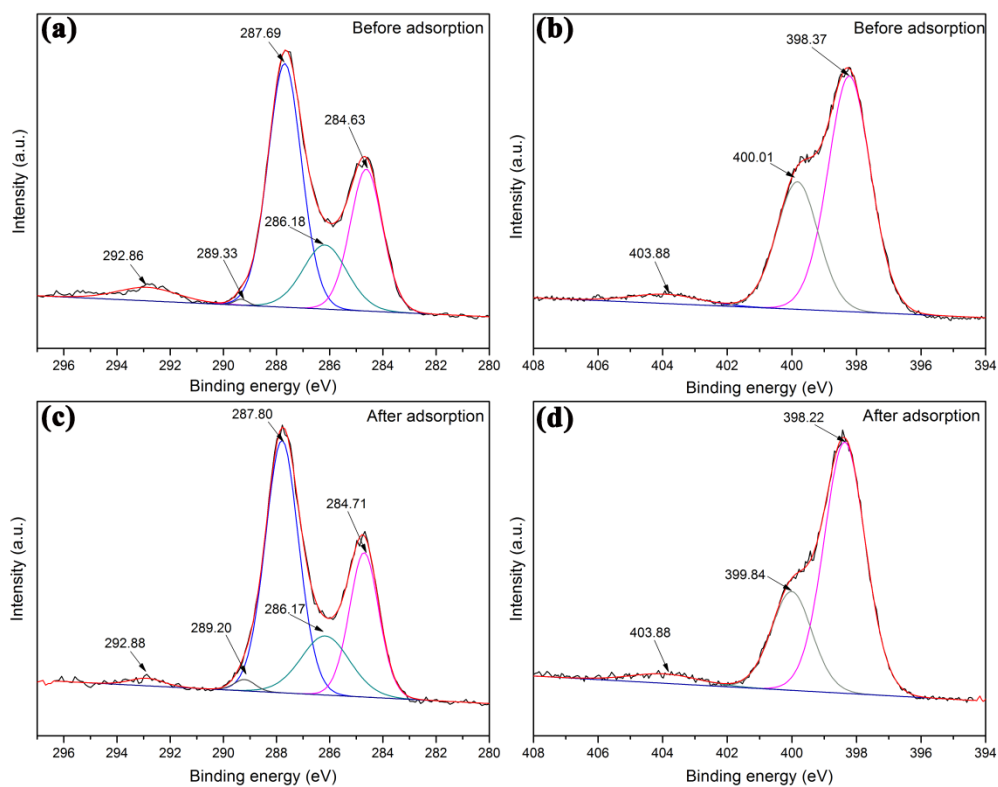


Figure S7. High resolution spectra of C 1s and N 1s before (a and b) and after (c and d) Pb adsorption on LiCl-CN-4h.

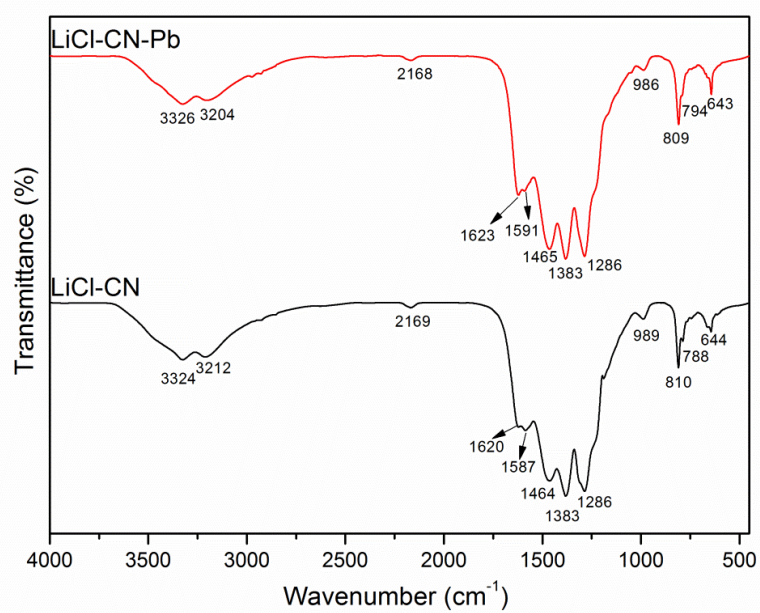


Figure S8. Infrared spectra of the as-prepared (a) and Pb²⁺-adsorbed LiCl-CN-4h (b).

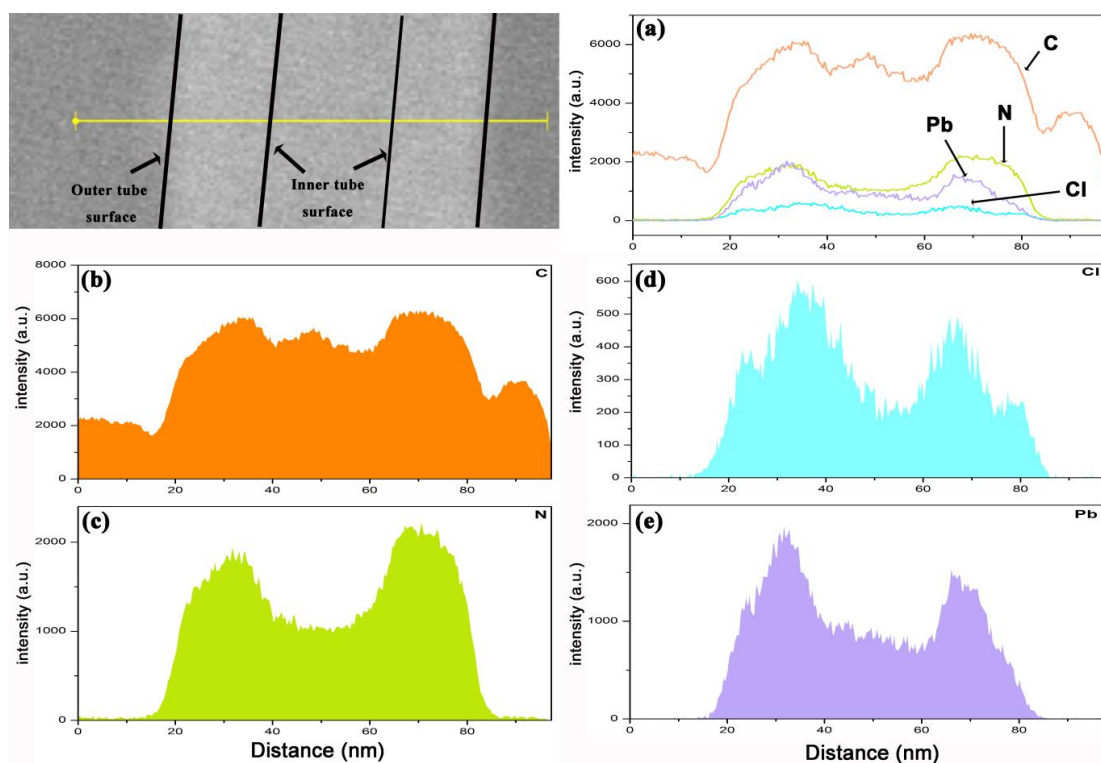


Figure S9. TEM-EDX line-scan profiles of the elements (a), together with the individual elemental distributions of C (b), N (c), Cl (d) and Pb (e) across the hollow tube after adsorption.

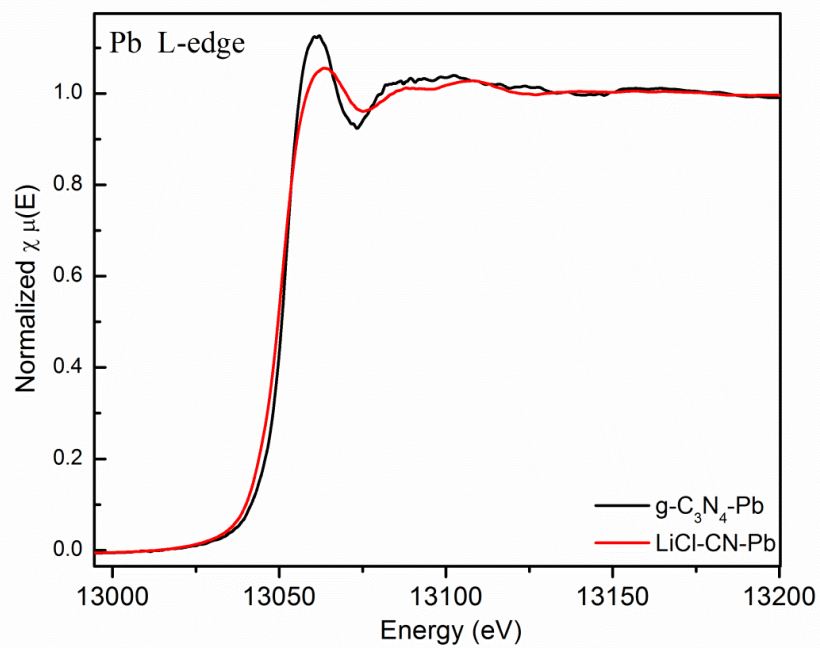


Figure S10. Pb L3-edge XANES spectra for samples after Pb²⁺ treatment.